18thBrazilian Congress of Thermal Sciences and Engineering
November 16-20, 2020, (Online)

ENC-2020-0232
PARTIALLY SATURATED METHOD FOR TWO-DIMENSIONAL FLUID FLOW PAST OBSTACLES

Evani Mollossi Porto
Pontifical University Catholic of Parana PUC-PR, rua Imaculada Conceição 1155, Prado Velho, Curitiba, PR, Brazil
evani.mollossi@gmail.com
Stephan Hennings Och
Federal University of Parana – UFPR, rua Cel. Francisco Heráclito dos Santos, 100 - Jardim das Américas, Curitiba, PR, Brazil
stephan.hennings.och@gmail.com
Paulo Cesar Philippi
Pontifical University Catholic of Parana PUC-PR, rua Imaculada Conceição 1155, Prado Velho, Curitiba, PR, Brazil
philippi@Impt.ufsc.br,

Abstract: *In several engineering applications such as automobiles aerodynamics, drag and lift coefficients are important to be determined. One method to preview the fluid flow effects is the use of computational simulation methods. The Lattice-Boltzmann Method (LBM) is one of them. It has been researched and used as a theoretical fluid mechanics simulation method. Based on widely accepted mesoscopic theories the LBM model is considered suitable to simulate physical phenomena in several areas, such as compressible and incompressible flows, micro fluid dynamics, porous media flow, hemodynamics and turbulence. In this paper we aim to investigate the application of the LBM with a variation of the standard method by the application of the Partially Saturated Method (PSM), to simulate an incompressible single phase fluid flow past obstacles in a two-dimensional model using a D2Q9 scheme (two dimensions and nine velocity vectors). The simulation is performed with the Reynolds number varying from 10 to 100 to illustrate that an obstacle may be subject to fluctuations in drag and lift forces as the magnitude of the Reynolds number increases. Results regarding drag forces and lift effects are compared with studies available in the literature and a good agreement were found in comparison with experimental and simulated data.*

Key words: Lattice Boltzmann Method, D2Q9, fluid flow past obstacles.

1. INTRODUCTION:

It is important to evaluate the aerodynamic effects, drag and lift forces, in external flow engineering applications. When such effects are not considered during the developments, the reliability of the final product may be reduced . As an example of such unfortunate case is the Tacoma Narrows Bridge in Washington – USA, inaugurated in July 1st 1940, it came to fail four months later its opening due torsional effects on its structure caused by air flow during a thunderstorm event (Washington State Department of Transportation, 2005). In the automobilist context, commercial vehicles travelling at 100 km/h have a consumption around 52 % of the total fuel used by the engine to provide power only to win the aerodynamic resistance, and considering that such vehicle might achieve 160.000 kilometers annually, reductions in aerodynamic drag may result in economy of fuel and decrease the emission of polluting gases (Moria *et al*., 2013).

Experimental investigation can be used to assist the development of aerodynamic solutions. As an alternative or complementary method, the use of electronic computers as flow simulators began in the 1950s. These computational simulation tools that generated the field of Computational Fluid Dynamics (CFD) appeared to numerically solve the equations that describe fluid flow and to simulate fluid mechanics in different problems (Ferziger, J. H. 2002).

An *alternative* method for fluid flow simulation is the Lattice Boltzmann model. Based on microscopic models and mesoscopic kinetic equations, the scheme showed to be successful in applications involving interfacial dynamics and complex boundaries. The central idea of this kinetic model to simulate macroscopic fluid flows is that the macroscopic dynamics of fluid is the result of collective behavior of many microscopic particles (Chen and Doolen, 1998)

Surmas R.(2004a) in his article, showed that the use of lattice Boltzmann in such problems as fluid flow simulation has advantages: it is very easy to program, and the method is intrinsically parallel. Also, an important advantage of the LB method regarding classical CFD methods is the needless of numerical derivatives of the velocity field to obtain the drag force. In summary, due to its mesoscale nature, the drag force can be obtained by considering the momentum exchanged between the lattice particles and the solid body.

The main objective of this work, is to validate a fluid flow simulation code based on LBM method for incompressible external flow with addition of the PSM method (Noble and Torczynski, 1998a) for treatment of the boundaries around obstacles. It is expected that the computational code developed is employable for flow analysis in two-dimensional flows and get more accurate results with application of the PSM method in comparison with results obtained with standard LBM method. The appearance of vortex just behind a solid obstacle that is placed against it is , also analyzed. When *Re* is greater than 45, the flow pattern becomes mechanically unstable and vortices are shed off by the main flow, forming the von Karmann vortex street (Lange *et al*., 1998a).

2. LATTICE BOLTZMANN METHOD (LBM)

Numerical simulations presented in this paper are based on a discretized form of the Maxell-Boltzmann equilibrium distribution of particles, the Lattice Boltzmann Equation (LBE) in a D2Q9 scheme (2 dimensions and 9 lattice vectors) in a grid of 500 x 1200 lattice sites. Each site is composed by 9 populations of particles (f_i), distributed among the four principal directions (e_1, e_2, e_3, e_4), the four diagonals directions (e_5, e_6, e_7, e_8) . A 9th population is at rest.

Figures 1 and 2 below illustrate the scheme and the 9 lattice vectors for each single site:

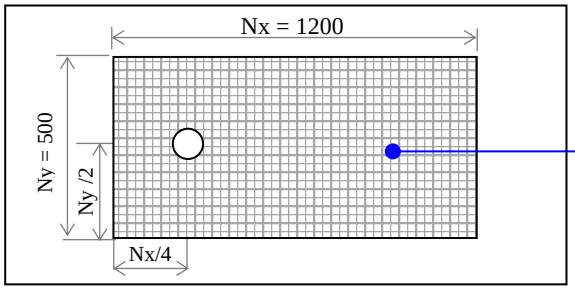

Figure 1. Scheme of 500 x 1200 lattices with an obstacle

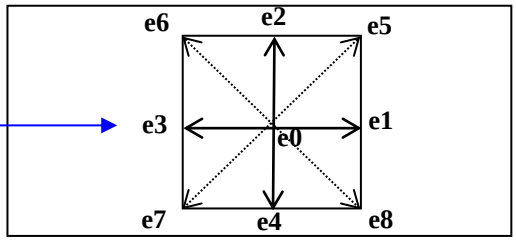

Figure 2. Nine particle distribution vectors of a lattice site

The equilibrium populations for each site are calculated as (He and Luo, 1997):

$$\bar{f}_i^{eq} = W_i \cdot \rho^* \left[1 + \frac{u_\alpha^* e_{i\alpha}}{c_s^2} + \frac{1}{2c_s^4} u_\alpha^* u_\beta^* (e_{i\alpha} e_{i\beta} - c_s^2 \delta_{\alpha\beta})\right], \quad (1)$$

where, in Eq. 1, ρ^* is the dimensionless number density of particles, W_i the quadrature weights that are dependent on the energy level, $W_0 = 4/9$, $W_{1,2,3,4} = 1/9$ and $W_{5,6,7,8} = 1/36$. Symbol u means the dimensionless macroscopic velocity, the term e_i is the scheme unitary velocity vectors $e_i = \{(0, 0), (1, 0), (0, 1), (-1, 0), (0, -1), (1, 1), (-1, 1), (-1,-1), (1,-1)\}$. Symbol c_s is used to indicate the discrete sound speed with value of $1/\sqrt{3}$ and δ the time step interval.

2.1 Collisions between particles

The populations referring to particle collisions are calculated at each site using the BGK collision operator model at each local information at time *t* (Bhatnagar et al., 1954):

$$\bar{f}_i^{out}(x, t + \delta) = \bar{f}_i(x, t) + \frac{\bar{f}_i^{eq}(x,t) - \bar{f}_i(x,t)}{\tau^*}, \quad (2)$$

where τ* is the value of the dimensionless relaxation term. The lower limit value for τ* is 1/2. In the case where τ* is ≤ 1/2 the numerical calculation becomes unstable. The term $\bar{f}_i^{eq}$ is calculated with Eq. (1) after the streaming step. The Reynolds number is calculated from the diameter of the obstacle *D* and discrete velocity *U* at the entrance of numerical domain (Surmas R., 2004b):

$$Re = \frac{UD}{\nu}, \quad (3)$$

where ν the dimensionless kinematic viscosity, which is related to relaxation time τ by:

$$\nu = {c_s}^2 \left(\tau - \frac{1}{2}\right). \quad (4)$$

2.2 Storage of calculated particles

In this step, the populations that were calculated previously are stored because in the next step they will change, and in the subsequent calculation of the forces exerted on the obstacles, the stored values of the populations are used:

$$f_{store} = \bar{f}_i^{out} . \tag{5}$$

2.3 Collisions on solid

The halfway bounce-back step is applied to make a rotation of fluid particles that are colliding on the solid. We consider the particles streaming half of the link distance between a neighbor to a solid site, and come back in opposite direction as follows (Ladd A., 1994):

$$f_i(x, y, t + \delta) = f_{-i}(x, y, t) , \tag{6}$$

After collision, the standard directions (0, 1, 2, 3, 4, 5, 6, 7, 8) are rotated and assumes the opposite values (0, 3, 4, 1, 2, 7, 8, 5, 6). Figure 3 below illustrates one single direction that collides on solid at time t + Δt/2 and come back in opposite direction at time t + Δt:

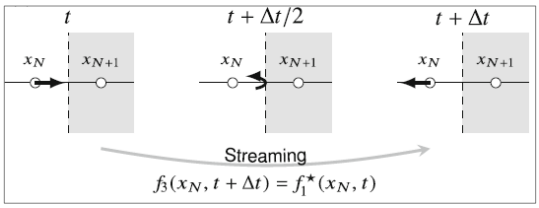

Figure 3. Half-way bounce back step (Krüger, T. et al 2017b).

The drag and lift forces (F_x, F_y), and their coefficients (*Cd*, *Cl*) are given by the equations 7, 8 and 9 below for the sites neighboring the solid (J. Meneghini *et al*., 2001):

$$F = \sum_{(n)} \sum_i (\bar{f}_{i)}(t) + \bar{f}_{(-i)}(t + \delta))e_i , \tag{7}$$

$$Cd(t) = \frac{2Fx(t)}{\rho U^2 D} , \tag{8}$$

$$Cl(t) = \frac{2Fy(t)}{\rho U^2 D} . \tag{9}$$

When the flow pattern becomes mechanically unstable in cases of Re greater than 45, vortices are shed off by the main flow, forming the von Karmann vortex street (Lange et al., 1998b). This effect causes oscillations on lift forces that enables to calculate the Strouhal number, that is a dimensionless frequency of vortices shedding behind body (Silva et al., 2003):

$$St = \frac{fD}{U} , \tag{10}$$

where f is the vortex shedding frequency calculated by a Fast Fourier Transform of the lift coefficient number *Cl*.

2.4 Calculation of number density of particles and velocity

The number density of particles (ρ*)and the dimensionless velocity of each site are calculated for all fluid sites, except for the domain contours in terms of the particle distribution function as shown below (Zou and He, 1997):

$$\rho^* = \sum_{i=0}^{8} \bar{f}_i , \tag{11}$$

$$\rho^* u_x^* = \sum_{i=1}^{8} \bar{f}_i \, e_{ix} , \tag{12}$$

$$\rho^* u_y^* = \sum_{i=1}^{8} \bar{f}_i \, e_{iy} . \tag{13}$$

3. PARTIALLY SATURATED METHOD FOR STAIRCASE SMOOTHING

The simulation scheme is composed by square sites for each lattice cell, which generates a staircase at the circumference of a circular obstacle. The PSM method also known as grey LBM or continuous bounce-back, treats this staircase by firstly calculating the solid fraction(ϵ) of each cell that varies from 0 to 1 as follows on Fig. 4 below:

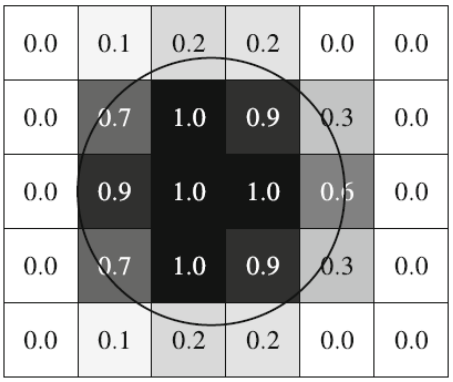

Figure 4. Solid fraction $0 \leq \epsilon < 1$ (Krüger, *et al* 2017c).

The idea is to smooth the shape details of the staircase lattice boundary nodes and to use a solid lattice volume fraction instead. The PSM main function consists in the use of a modified BGK collision term, where, may be considered like LBM with addition of friction force that varies locally depending on the nodal solid/fluid fraction (Noble and Torczynski, 1998b).

$$f_i(x + c_i\,\Delta t, t + \Delta t) = f_i(x,t) + (1-B)\Omega_I^f + B\Omega_I^s\ . \tag{14}$$

The term *B* is a weighting parameter given by:

$$B(\epsilon,\tau) = \frac{\epsilon(\tau - \frac{1}{2})}{(1-\epsilon)+(\tau - \frac{1}{2})}\ . \tag{15}$$

It can be seen that *B* increases when ϵ varies from 0 (pure fluid) to 1 (pure solid) for any value of $\tau > \frac{1}{2}$.
The term Ω_I^f in (14) is the standard BGK collision operator for fluid (*f*) nodes:

$$\Omega_I^f\ = \frac{f_i^{eq}(x,t) - f_i(x,t)}{\tau}. \tag{16}$$

The term Ω_I^s in (14) is the standard BGK collision operator for solid (*s*) nodes:

$$\Omega_I^s\ = \left(f_{\bar{i}}(x,t) - f_{\bar{i}}^{eq}(\rho,\boldsymbol{u})\right) - \left(f_i(x,t) - f_i^{eq}(\rho,\boldsymbol{u}_s)\right), \tag{17}$$

where $f_{\bar{i}}$ is the post returned populations after collision on solid, $\boldsymbol{u}$ the fluid velocity and $\boldsymbol{u}_s$ the speed at the solid nodes.

4. RESULTS

The drag and lift coefficients obtained in the present work are compared with those of other contemporary authors using CFD and LBM. Accuracy is seen by the comparison evaluation analysis. Tab. 1 and Fig. 5 shows the results of

contemporary authors compared with the results of the present work. Drag coefficient (Cd) obained by LBM method with standard BGK collision operator and PSM with modified BGK were found to be in accordance with literature. Improvement is obtained with PSM method:

Table 1. Comparison results for drag coefficient around cylinder with different authors. Reynolds number varying from 10 to 100.

Method	Author	Drag coefficient					
		Re 10	Re 20	Re 40	Re 60	Re 80	Re 100
Exp.	Triton (1959) - experiment	3.07	2.09 (Re 19)	1.46 (Re 38)	1.47	1.32 (Re 78)	1.26 (Re 97)
CFD	Dennis and Chang, (1970)	2.846	2.045	1.522	-	-	1.056
	Park et al., (1998)	2.780	2.010	1.510	1.39	1.35	1.330
	Qu et al (2013) - Finite Volume	-	-	-	1.38	1.33	1.32
LBM	He and Doolen (1997)	3.170	2.152	1.499	-	-	-
	Surmas *et al.*, (2004c)	2.8	2	1.5	1.5	1.4	1.4
	Guo and Shu, (2013)	2.942	2.155	1.604	-	-	-
	Present work [(1)] standard BGK	3.178	2.257	1.676	1.496	1.434	1.413
	Present work modified BGK (PSM method)	2.969	2.080	1.544	1.398	1.353	1.334

[(1)] Simulations with LBM using cylinder diameter (D) with 40 lattice sites and dimensionless macroscopic velocity (u) equals to 0.04 at the entrance of numerical domain.

Fig. 5 below shows the drag coefficient results of the present work described on Tab. 1. It can be seen a better agreement with PSM method in comparison with experimental data and results of contemporary authors:

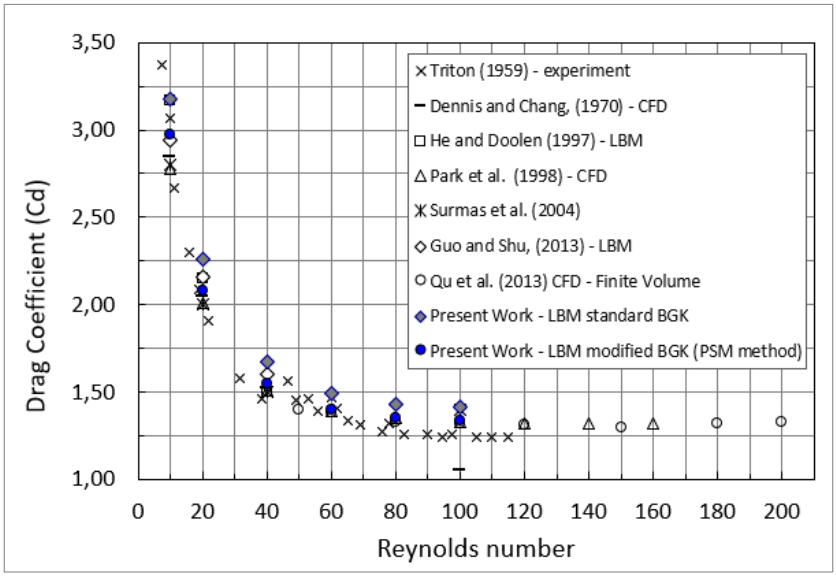

Figure 5. Drag coefficients results of present work in comparison with literature data.

Fig. 6 shows the St results of the present work in comparison with experimental data and results of contemporary authors. It can be seen a good agreement with reference data:

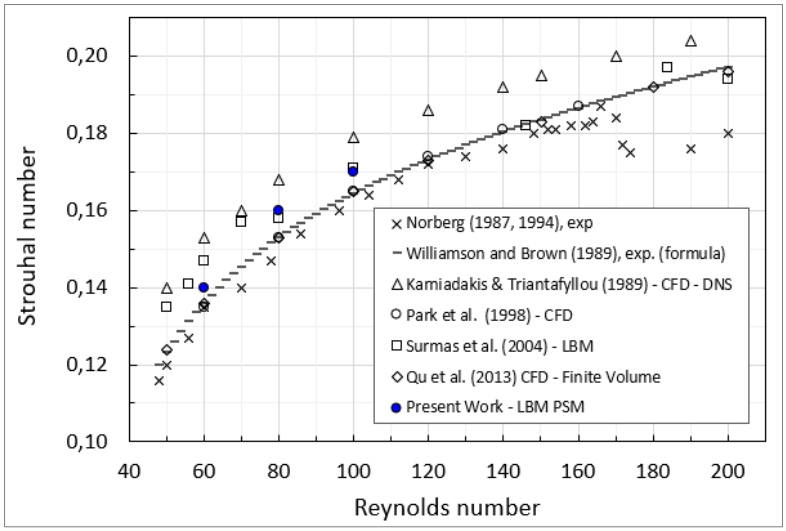

Figure 6. Strouhal number results of the present work in comparison with literature data.

Fig. 7 below shows the discretized dimensionless velocity field around a cylinder where is possible to see the vortices street behind cylinder. On Fig. 8 the respective drag and lift coefficients are shown, where is possible to identify a bigger oscillation on Cl with a mean value around zero and a smaller variation on Cd, with mean value around 1.33. These results were obtained in the present work with the modified BGK (PSM method) for Re 100:

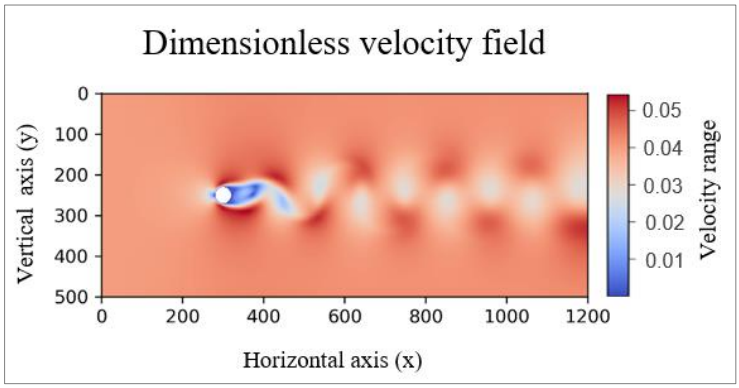

Figure 7. Discretized dimensionless velocity field with Vortex Street upstream obstacle (Re = 100)

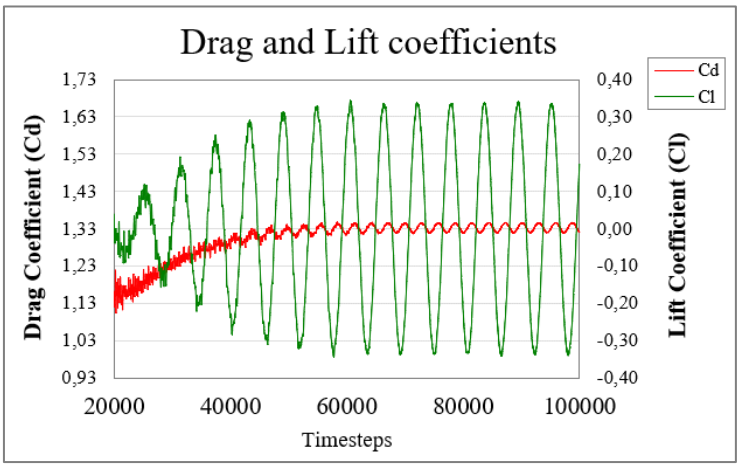

Figure 8. Drag and Lift coefficients for (Re = 100), Cd mean: 1.334, Cl mean: -0.04, Cl p-p: ± 0.32

5. CONCLUSION

The main purpose of this paper was to produce a benchmark in order to assess the relative performance of smoothing when performing LB numerical simulations of flows past solid bodies. For this purpose, the partially saturated method of Noble and Torczynski, 1998b was used. Results are in good agreement with the results available in the literature from simulations performed by other authors based on CFD traditional methods. Applying the PSM method to smooth the staircase on solid surfaces avoids increasing the numerical domain resolution. Considering that this resolution increase has a significant impact on computational costs, the method can be considered as a fair alternative to save expenses on computational simulations.

6. REFERENCES

Bhatnagar,P.L., GrossE.P., KrookM., 1954, A model for collision processes in gases. I. Small amplitude processes in charged and neutral one-component system, Phys. Rev. 94 pp. 511–525.

Chen S. and Doolen, G. D., 1998, Lattice Boltzmann Method for Fluid Flows, Annu. Rev. Fluid Mech. 30: pp. 329–364

Dennis, S.C.R. and Chang, G., 1970, Numerical solutions for steady flow past a circular cylinder at Reynolds numbers up to 100, Journal of Fluid Mechanics 42 pp. 471.

Ferziger, J. H., 2002. Computational Methods for Fluid Dynamics. New York,: Springer.

Guo, Z. and Shu, C., 2013. Lattice Boltzmann Method and its application in Engineering. Singapore: World Scientific Publishing Co. Pte. Ltd. Vol 3.

He. X. and L.S. Luo, 1997, Theory of lattice Boltzmann method: from the Boltzmann equation to the lattice Boltzmann equation, Phys. Rev. E 56 pp. 6811–6817.

He, X. and Doolen, G. 1997, Lattice-Boltzman Method on Curvilinear Coordinates System: Flow Around a Circular Cylinder. J. Compt. Phys, 134, pp. 306-315.

Karniadakis, G., Triantafyllous, G. S., 1989, Frequency selection and asymptotic states in laminar wakes, J . Fluid Mech. vol. 199, p p . 441-469

Krüger, T. et al, 2017, The Lattice Boltzmann Method, Principles and Practice. Switzerland: Springer International Publishing.

Ladd,A.J.C., 1994,Numerical simulations of particulate suspensions via a discretized Boltzmann equation. Part 1. Theoretical foundation", J. Fluid Mech. 271, pp. 285-309.

Lange,C.F., 1998, DurstF., BreuerM., Momentum and heat transfer from cylinders in laminar crossflow at $10{-}4 \leq Re \leq 200$, Int. J. Heat Mass Transf. 41, pp. 3409–3430.

McNamara, G. R. and Zanetti G., Use of the Boltzmann Equation to Simulate Lattice-Gas Automata, Physical Review Letters 61(20), pp. 2332-2335.

Meneghini, J.R., SaltaraF., SiqueiraC.L.R., FerrariJ.A. Jr., 2001, Numerical simulation of flow interference between two circular cylinders in tandem and side-by-side arrangements, Journal of Fluids and Structures 15, pp. 327 – 350.

Moria, H.. 2013, A study on aerodynamic drag of a semi-trailer truck. Science Direct 56, pp. 201-205.

Noble, D.R., Torczynski, J.R., 1998, A Lattice-Boltzmann Method for Partially Saturated Computational Cells, International Journal of Modern Physics C, Vol. 9, No. 8, pp. 1189-1201

Norberg, C. 1994, An experimental investigation of the flow around a circular cylinder : influence of aspect ratio, J . Fluid Mech., vol. 258, pp. 287-316

Park,J.; Kwon, K.; Choi,H. (1998) Numerical solutions of flow past a circular cylinder at Reynolds number up to 160, KSME International Journal Vol. 12, Nº 6, pp. 1200-1205.

Qu, L. ; Norberg, C. ; Davidson, L. (2013) "Quantitative numerical analysis of flow past a circular cylinder at Reynolds number between 50 and 200". Journal of Fluids and Structures, vol. 39 pp. 347-370.

Silva, L. E., A.L.F. Lima; Silveira-Neto, A; Damasceno, J.J.R,2003,Numerical simulation of two-dimensional flows over a circular cylinder using the immersed boundary method. Journal of Computational Physics 189, pp. 351–370.

Surmas, R. 2004, Lattice Boltzmann simulation of the flow interference in bluff body wakes. Science Direct, Future Generation Computer Systems 20 (2004), pp. 951–958.

Tritton, D. J., 1959, Experiments on the flow past a circular cylinder at low Reynolds numbers, Journal of Fluids Mechanics, Volume 6, Issue 4, PP 547-567

Washington State Department of Transportation. (2005). Tacoma Narrows Bridge. Access on October 13th 2019, available in Washington State Department of Transportation:https://www.wsdot.wa.gov/TNBhistory/Machine/machine3.htm

Williamson, C. H. K., 1988. The existence of two stages in the transition to three-dimensionality of a cylinder wake. Physics of Fluids, vol 31 (11), pp. 3165–3168.

Williamson, C. H. K., 1989. Oblique and parallel modes of vortex shedding in the wake of a circular cylinder at low Reynolds numbers. Journal of Fluid Mechanics, vol 206, pp. 579–627.

Williamson, C. H. K., 1996, Vortes Dynamics in the cylinder wake, Annual Reviews Fluid. Mech. vol. 28 pp. 477-539

Zou,Q., He, X.,1997, On pressure and velocity boundary conditions for the lattice Boltzmann BGK model, Physics of Fluids 9, 1591

7. RESPONSIBILITY NOTICE

The authorsare the only responsible for the printed material included in this paper.